Comparison of 4*H*-SiC impact ionization models using experiments and self-consistent simulations

Akin Akturk,[1,a)] Neil Goldsman,[1] Shahid Aslam,[2] John Sigwarth,[2] and Fred Herrero[2]
[1]*Electrical and Computer Engineering, University of Maryland, College Park, Maryland 20742, USA and CoolCAD Electronics, Takoma Park, Maryland 20912, USA*
[2]*NASA Goddard Space Flight Center, Greenbelt, Maryland 20771, USA*

(Received 13 May 2008; accepted 21 May 2008; published online 23 July 2008)

We report comparisons of measured photocurrent versus voltage curves of avalanche photodiodes (APDs) with those calculated using different 4*H*-SiC hole and electron impact ionization coefficients. As the published impact ionization coefficients result in ionization rates that differ greatly in magnitude, the predicted breakdown voltages using these models vary by many volts. To this end, we investigate the breakdown voltage prediction capability of three prevailing impact ionization models in conjunction with several experiments. To obtain APD performance numerically, we developed a device simulator, which shows that the inclusion of proper electric field-dependent impact ionization rates can accurately predict a variety of measured current-voltage curves, breakdown voltages, and current multiplication rates. © *2008 American Institute of Physics*.
[DOI: 10.1063/1.2958320]

SiC polytypes and especially 4*H*-SiC are finding ever-increasing uses in power electronic components such as thyristors and power metal-oxide- semiconductor field-effect transistors due to their large bandgaps, high breakdown fields, high thermal conductivities, low leakage currents, low intrinsic noise figures, and relatively mature fabrication methods compared to other wide-bandgap materials. 4*H*-SiC is also a material of choice for solar-blind ultraviolet (UV) photodetectors with its inherent favorable material properties such as transparency to the sun's visible spectrum, high sensitivity to photons while maintaining low dark current levels, stability at high temperatures, and radiation-hardness. In power applications, 4*H*-SiC devices block hundreds of volts in their off-states with minimal leakage currents up to the safe operating voltage limits that are dictated by the device breakdown mainly due to the impact ionization. Further, to increase sensitivity and signal-to-noise ratios in 4*H*-SiC UV detectors for resolving low photon fluxes, the devices are operated in avalanche multiplication mode near breakdown voltages (BVs), where gains and consequently output currents are high. Thus to obtain performance and reliability limits of these 4*H*-SiC devices, the use of predictive carrier impact ionization rates is important as the device operation is very sensitive to these rates.

We develop device simulators to investigate effects of different impact ionization rates on device performance and use them to examine the operation of 4*H*-SiC avalanche photodiodes (APDs) since the impact ionization is the dominant mechanism that determines the APD performance. To investigate the operation of 4*H*-SiC avalanche diodes, we build on our previous work[1–3] and develop a physics-based diode simulator that self-consistently solves for Poisson's equation, electron current continuity equation, and hole current continuity equation following, respectively,

$$\nabla^2\phi = -\frac{q}{\varepsilon}(p - n + D), \tag{1}$$

$$\frac{\partial n}{\partial t} = \nabla\cdot(-n\mu_n\nabla\phi + \mu_n V_{\text{th}}\nabla n) + G_{\text{t}} + G_{\text{ii}} + G_{\text{op}}, \tag{2}$$

$$\frac{\partial p}{\partial t} = \nabla\cdot(p\mu_p\nabla\phi + \mu_p V_{\text{th}}\nabla p) + G_{\text{t}} + G_{\text{ii}} + G_{\text{op}}. \tag{3}$$

Above, n is the electron concentration, p is the hole concentration, ϕ is the electrostatic potential, D is the net dopant concentration, μ is the mobility, V_{th} is the thermal voltage, G_{t} is the Shockley–Read–Hall generation-recombination term, G_{ii} is the impact ionization rate, G_{op} is the optical generation rate, q is the electronic charge, and ϵ is the dielectric constant.

Here, we focus on the impact ionization rate. To obtain photocurrent versus reverse bias voltage curves of APDs and their BVs, we employ three different published 4*H*-SiC impact ionization rate models for the (0001) direction.

Model 1. It uses nonstandard exponential type impact ionization rate expressions[4] with the exponents that are functions of a multiple of the 4*H*-SiC optical phonon energy (ξ_o=0.36 eV), the carrier ionization energies (ξ_i^p =7 eV, ξ_i^n=10 eV), and the electron/hole mean free paths (λ_p=3.25 nm, λ_n=2.99 nm) in addition to the local electric field (E). Also the coefficient in front of the exponential is a function of the electric field as shown below for holes (β_{ii}) and electrons (α_{ii}),

$$\beta_{\text{ii}} = \left(\frac{qE}{\xi_i^p}\right)\exp\left[-\frac{\xi_i^p\xi_o}{qE\lambda_p(\xi_o + qE\lambda_p)}\right], \tag{4}$$

$$\alpha_{\text{ii}} = \left(\frac{qE}{\xi_i^n}\right)\exp\left[-\frac{\xi_i^n\xi_o}{(qE\lambda_n)^2}\right]. \tag{5}$$

Model 2. These impact ionization rate expressions[5] written

[a)]Electronic mail: akturka@umd.edu.

 © 2008 American Institute of Physics

Downloaded 04 Mar 2011 to 128.183.169.235. Redistribution subject to AIP license or copyright; see http://jap.aip.org/about/rights_and_permissions

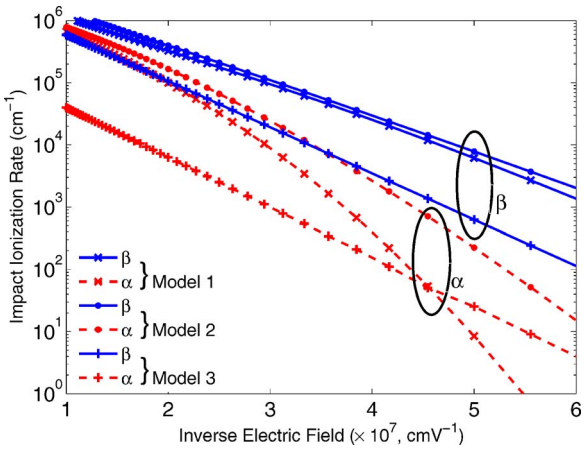

FIG. 1. (Color online) Field-dependent impact ionization rates for holes (β_{ii}) and electrons (α_{ii}) using three different models.

below are similar to the standard formulas, except for the powers in the exponents. Here, the multiplicative coefficients are $a_p = 4.38 \times 10^6$ cm^{-1} and $a_n = 1.98 \times 10^6$ cm^{-1}, the critical electric fields are $E_c^p = 1.14 \times 10^7$ V cm^{-1} and $E_c^n = 9.46 \times 10^6$ V cm^{-1}, and the powers are $\gamma_p = 1.06$ and $\gamma_n = 1.42$,

$$\beta_{ii} = a_p \exp\left[-\left(\frac{E_c^p}{E}\right)^{\gamma_p}\right], \tag{6}$$

$$\alpha_{ii} = a_n \exp\left[-\left(\frac{E_c^n}{E}\right)^{\gamma_n}\right]. \tag{7}$$

Model 3. This model employs standard exponential field-dependent impact ionization rates,[6,7] where the coefficients in front of the exponentials are constants and the exponents only linearly depend on the inverse electric field. In this model, the impact ionization rate formulas are similar to those in Eqs. (6) and (7) with the exponentials multiplied by $a_p = 3.25 \times 10^6$ cm^{-1} and $a_n = 2.5 \times 10^5$ cm^{-1}, the critical fields taken as $E_c^p = 1.71 \times 10^7$ V cm^{-1} and $E_c^n = 1.84 \times 10^7$ V cm^{-1}, and the powers set to $\gamma_p = 1$ and $\gamma_n = 1$.

We then calculate the local electron/hole generation rate due to impact ionization using one of the three sets of the preceding impact ionization rates, plotted in Fig. 1, and the current densities $J_n = q|-n\mu_n \nabla \phi + \mu_n V_{\text{th}} \nabla n|$ and $J_p = q|p\mu_p \nabla \phi + \mu_p V_{\text{th}} \nabla p|$ as follows:

$$G_{\text{ii}} = \frac{1}{q}(\beta_{\text{ii}} J_p + \alpha_{ii} J_n). \tag{8}$$

Numerical challenges in 4*H*-SiC APD simulations are mainly related to its low intrinsic carrier concentration (7×10^{-9} cm^{-3} at room temperature) at the material level, and the choice of carrier boundary conditions under optical illumination and the resolution of avalanche breakdown at the device level. We develop numerical techniques to overcome the first two challenges. The electron and hole concentrations at the boundaries, which are in excess of those in thermal equilibrium, are updated by taking the volume integral of the current continuity equations over the device volume and considering that the excess charge causes an additional diffusion current at the terminals.

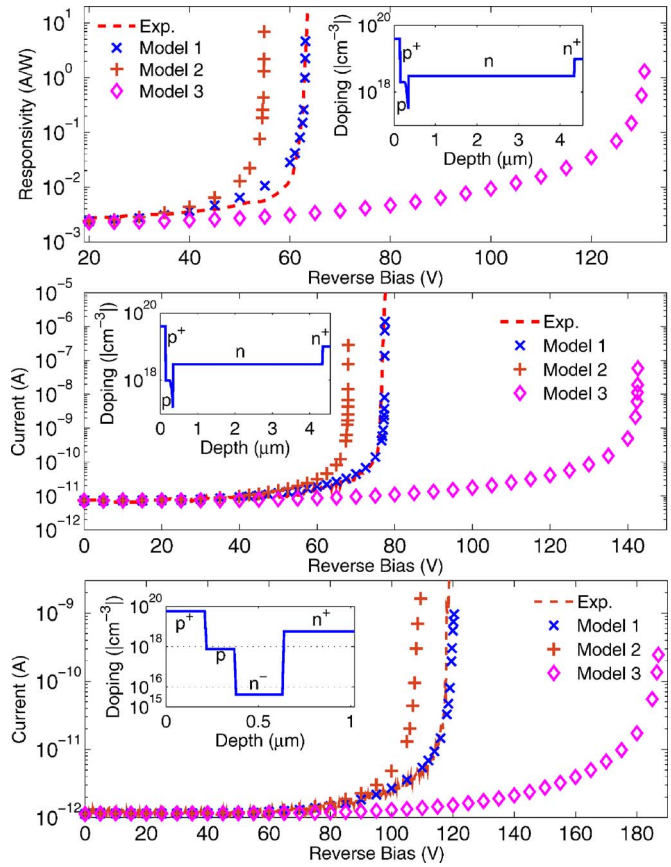

FIG. 2. (Color online) Measured and calculated reverse voltage dependent responsivity curves of (a) (top) a low-noise 4*H*-SiC APD (Ref. 8) along with photocurrent curves of (b) (middle) a single-photon counter 4*H*-SiC APD (Ref. 9) and (c) (bottom) a high-performance 4*H*-SiC APD (Refs. 10 and 11).

To investigate the effects of different impact ionization rates on calculated results, we start with a low-noise 4*H*-SiC APD that incorporates a 0.1 μm long p^+ (4×10^{19}), a 0.2 μm long p (2×10^{18}–2×10^{17}), a 2.0 μm long n (3×10^{18}), and a 0.5 μm long n^+ (1×10^{19}), respectively, as described in Ref. 8. We calculate the responsivity at 320 nm, where the absorption coefficient is approximately 2500 cm^{-1}, using the three aforementioned models. Figure 2(a) shows that the first model predicts the measured curve as well as the measured BV, whereas the high ionization rates associated with the second model underestimates the BV while the low ionization rates of the third model greatly overestimates it. We then compare our calculated results with those in Ref. 9, as shown in Fig. 2(b). We assume a similar doping profile except for the p layer, whose doping is halved compared to the previous case, between p^+ and n, and the incident photon wavelength from now on assumed approximately 280 nm with 2×10^4 cm^{-1} as roughly the absorption coefficient. Model 1 predicts the current level and the BV as well as the transitional current region around the onset of the breakdown. A similar trend between measured and calculated results follows in Fig. 2(c), which shows recently measured results of the works of Xin *et al.*[10] and Gaskill *et al.*[11] for an APD that incorporates a 0.22 μm long p^+ (6×10^{19}), a 0.16 μm long p (7.5×10^{17}), a 0.26 μm long n (4×10^{15}), and a 0.38 μm long n^+ (5.8×10^{18}), respectively. Likewise,

Downloaded 04 Mar 2011 to 128.183.169.235. Redistribution subject to AIP license or copyright; see http://jap.aip.org/about/rights_and_permissions

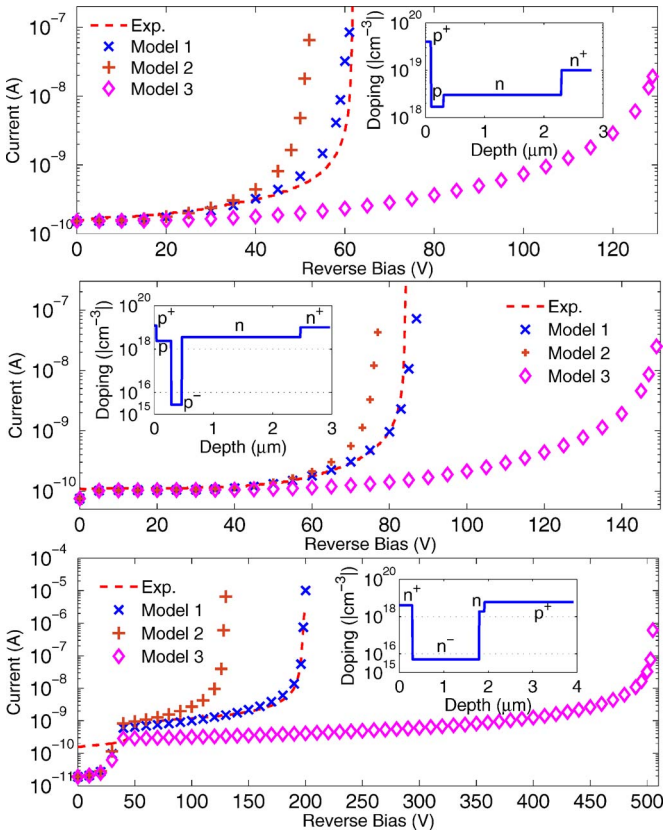

FIG. 3. (Color online) Measured and calculated photocurrent vs reverse voltage curves of 4*H*-SiC APDs [(a) top (Ref. 12), (b) middle (Ref. 14), and (c) bottom (Ref. 13)]. 4*H*-SiC APD in Ref. 13 incorporates separate absorption and multiplication regions.

a comparison of measured results in Refs. 12–14, respectively for Figs. 3(a)–3(c), indicate that the use of Model 1 for the 4*H*-SiC impact ionization rates successfully predicts a variety of measured data including the BVs, photocurrents, and responsivities. [We note that while slight changes in doping values are less influential on the BVs and currents for calculated data, the results are sensitive to dopings for the APD in Ref. 13 and Fig. 3(c).]

In conclusion, calculated 4*H*-SiC APD performances are greatly affected by the utilized impact ionization rates. Our numerical results along with several experimental data show that Model 1 is a predictive tool for use in device simulators. Moreover, the constants that are used in the model are linked to physical parameters and are beyond empirical fits. This feature might be useful in Monte Carlo-type transport simulations.

ACKNOWLEDGMENTS

This work was supported in part by the NASA GOES-R Flight Project and the NOAA GOES-R Program Office at the NASA Goddard Space Flight Center.

[1]S. Potbhare, N. Goldsman, G. Pennington, A. Leilis, and J. McGarrity, J. Appl. Phys. **100**, 044515 (2006).
[2]S. Potbhare, N. Goldsman, G. Pennington, A. Leilis, and J. McGarrity, J. Appl. Phys. **100**, 044516 (2006).
[3]A. Akturk, G. Pennington, and N. Goldsman, IEEE Trans. Electron Devices **52**, 577 (2005).
[4]A. O. Konstantinov, Q. Wahab, N. Nordell, and U. Lindefelt, Appl. Phys. Lett. **71**, 90 (1997).
[5]B. K. Ng, J. P. R. David, R. C. Tozer, G. J. Rees, F. Yang, J. H. Zhao, and M. Weiner, IEEE Trans. Electron Devices **50**, 1724 (2003).
[6]R. Raghunathan and B. J. Baliga, Proceedings of Power Semiconductor Devices and ICs (ISPSD), 1997 (unpublished), p. 173.
[7]R. Raghunathan and B. J. Baliga, Solid-State Electron. **43**, 199 (1999).
[8]F. Yan, C. Qin, J. H. Zhao, M. Weiner, B. K. Ng, J. P. R. David, and R. C. Tozer, Electron. Lett. **38**, 335 (2002).
[9]X. Xin, F. Yan, X. Sun, P. Alexandrove, C. M. Stahle, J. Hu, M. Matsumura, X. Li, M. Weiner, and H. J. Zhao, Electron. Lett. **41**, 212 (2005).
[10]X. Xin, J. Hu, P. Alexandrove, J. H. Zhao, B. L. VanMil, D. K. Gaskill, K. K. Lew, R. M. Ward, and C. Eddy, Proc. SPIE **6771**, 677114 (2007).
[11]K. Gaskill, B. VanMil, E. Glaser, K. Lew, R. Ward, C. Eddy, L. Wang, and P. Zhao, Proceedings of the MRS Spring 08, 2008 (unpublished), p. D12.4.
[12]J. C. Campbell, S. Demiguel, F. Ma, A. Beck, X. Guo, S. Wang, X. Zheng, X. Li, J. D. Beck, M. A. Kinch, A. Huntington, L. A. Coldren, J. Decobert, and N. Tscherptner, IEEE J. Sel. Top. Quantum Electron. **10**, 777 (2004).
[13]X. Guo, L. B. Rowland, G. T. Dunne, J. A. Fronheiser, P. M. Sandvik, A. L. Beck, and J. C. Campbell, IEEE Photonics Technol. Lett. **18**, 136 (2006).
[14]X. Guo, A. L. Beck, X. Li, J. C. Campbell, D. Emerson, and J. Sumakeris, Appl. Phys. Lett. **86**, 193103 (2005).

Downloaded 04 Mar 2011 to 128.183.169.235. Redistribution subject to AIP license or copyright; see http://jap.aip.org/about/rights_and_permissions